JTE
HCMUTE
ISSN: 2615-9740

JOURNAL OF TECHNICAL EDUCATION SCIENCE
Ho Chi Minh City University of Technology and Education
Website: https://jte.hcmute.edu.vn/index.php/jte/index
Email: jte@hcmute.edu.vn

Optimization Procedure for IPM Motor by Changing the Rotor Structure

Bui Duc Hung*, Bui Minh Dinh, Dang Quoc Vuong

School of Electrical and Electronic Engineering, Hanoi University of Science and Technology, Vietnam.

*Corresponding author. *Email: hung.buiduc@hust.edu.vn*

ARTICLE INFO

Received: 25/11/2022
Revised: 25/12/2022
Accepted: 28/12/2022
Published: 28/02/2023

KEYWORDS

Interior permagnent magnet motor;
Electromotive force (EMF);
Electromagnetic torque;
GA optimization;
IPM motor;
Finite element method.

ABSTRACT

The paper has developed an optimization procedure to design the rotor lamination and magnetic sizes. The average torque is improved by changing the thickness of the outer bridge and magnetic width. Various metamodels with the best prediction performance generated for each of the multi-objective functions and constraints have been selected. By applying a multi-objective genetic algorithm, several optimal solutions have to be considered to compare with those of the initial model. Hence, the multi-objective optimization method for designing the interior permanent magnet (IPM) motor is presented to obtain the high reliability and maximum torque. This development allows to estimate the back electromotive force (EMF), magnetic flux density and electromagnetic torque. In addition, the torque ripple evaluated via the analytical Matlab program is coupled to the finite element method and genetic algorithm optimization. Rotor laminations are finally stamped and assembled into the motor to verify the EMF under the rated load and no load test.

Doi: https://doi.org/10.54644/jte.75A.2023.1313

1. Introduction

Recently, many researchers have presented manner solutions to improve the electromagnetic torque and efficiency of electric motors. In [1], authors proposed a way of changing the rotor structure by inserting permanent magnets (PMs) into the squirrel cage rotor to improve the electromagnetic torque. In [2], authors concentrated on analyzing the electrometic parameters of IPM motor of 200kW-450 Nm to improve performances of the electric motor by using the finite element method (FEM). In [3], authors presented a method to analyse the electromagnetic and thermal problem of IPM motors by using filled slots and hairpin windings. In [4], a multi-objective optimization design method for the permanent magnet synchronous motor (PMSM) based on the artificial bee colony algorithm was proposed to obtain the high dynamic performance and high efficiency. In [5], authors developed a constrained multi-objective optimization design formulation for surface-mounted (SM) PMSM, where therein a rigorous multi-objective optimization problem was proposed for an integer-slot distributed-winding SM-PMSM. In [6], a novel memetic algorithm combined with mesh adaptive direct search for a PMSM was investigated.

In this paper, an optimization procedure has been proposed to maintain the out power as a constant in the field-weakening region of a three-phase interior permanent magnet (IPM) synchronous motor (IPMSM). The optimization design is performed via the development of the class of controlled random search (CRS) algorithms proposed in [5]-[8]. The multi-objective optimization of maximum average torque and output power is proposed to investigate an IPM motor of 5 kW, 8 poles and 24 slots. In this method, several parameters of the stator diameter, slot depth, air gap and magnet angle are variables. The development of the method will be applied to the middle drive motor and electrical cars.

2. Design variables and constrains

As presented, based on the stator, rotor diameter and power inverter of voltage and current, the electromagnetic torque (T) has been calculated as [5]-[9]:

$$T = \frac{\pi}{2} D^2 L_{stk} \sigma, \quad (1)$$

JTE
HCMUTE
ISSN: 2615-9740

JOURNAL OF TECHNICAL EDUCATION SCIENCE
Ho Chi Minh City University of Technology and Education
Website: https://jte.hcmute.edu.vn/index.php/jte/index
Email: jte@hcmute.edu.vn

where D is the rotor diameter, L_{stk} is the stack length of rotor and σ is the factor defined as $\sigma = \frac{L}{D}$. For the inner rotor, this factor value is from 0.8 to 1.25.

The prediction of torque is considered with different relative positions of the rotor and stator. When the rotor is rotated, the mesh is automatically adjusted. Hence, the influence of mesh on the rotor is investigated to analyze inaccuracies due to the element distortion. Based on that, it will show the satisfactory accuracy with a suitable mesh. Due to the symmetry of rotor structure, one pole is simulated.

The stator voltage equations at steady-state are written in the d-q axis [10]-[12]:

$$v_d = Ri_d - \omega L_q i_q, \tag{2}$$

$$v_q = Ri_q + \omega L_d i_d + \omega L_q i_q, \tag{3}$$

where R is the resistance of winding, L_d and L_q are respectively the direct and quadrature inductances, i_d and i_q are respectively the direct and quadrature armature currents. The quantities v_d and v_q are the terminal voltages of direct and quadrature components, respectively. The electromagnetic torque (T) is then defined as [13]-[16]

$$T = \frac{3}{2} p\left[\phi_M i_q + (L_d - L_q) i_d i_q\right], \tag{4}$$

where ϕ_M is the magnetic flux due to the permanent magnet which is linked to the armature winding.

As presented in Section I, a three-phase IPM motor of 5 kW, 8 poles and 24 slots is considered. Figure 1 shows a cross-section core of the stator and rotor. It can be seen that the permanent magnets are inserted into the flux barriers.

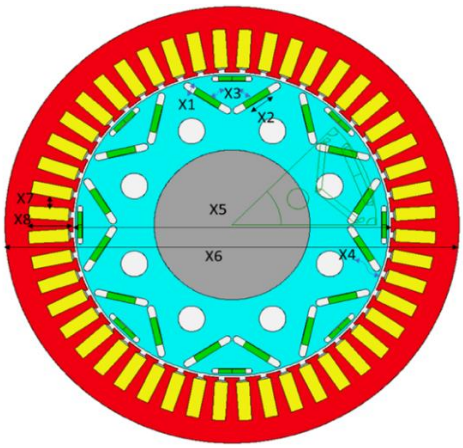

Figure 1. *Cross-section core of the stator and rotor.*

Both the rotor and stator are made by lamination stacks with high permeability non-oriented grain silicon steel. The windings using in this machine are the double-layer distributed windings. The optimization procedure with the set of parameters (x) is given in Table I.

Table 1. *Design variables with minimum and maximum ranges.*

Parameters	Discrete variables	min	max	step
L1 Magnet Thickness (mm)	x1	2	4	0.2
L1 Magnet Bar Width (mm)	x2	8	12	1
L1 Pole V Angle (deg)	x3	120	150	1
Airgap (mm)	x4	0.5	1.5	0.1
Stator Lam Dia (mm)	x5	130	150	1
Stator Bore (mm)	x6	70	90	1
Tooth Width (mm)	x7	4	6	0.2
Slot Depth (mm)	x8	16	20	0.4

JTE
HCMUTE
ISSN: 2615-9740

JOURNAL OF TECHNICAL EDUCATION SCIENCE
Ho Chi Minh City University of Technology and Education
Website: https://jte.hcmute.edu.vn/index.php/jte/index
Email: jte@hcmute.edu.vn

We can see that there are 8 variables in the proposed machine, i.e., from x1 to x8. These variables are performed in a discrete way. In order to obtain the high electromagnetic performances, the irreversible demagnetization has to be minimized. This means that under the high-speed operation, the mechanical stress on steel bridges has to be taken into account.

In order to give the final design, the optimization procedure has to be satisfied several constraints. Firstly, the value of the back electromagnetic force (EMF) at the maximum speed is not allowed to be bigger than the rated terminal voltage with the maximum current density. Secondly, the constraints for inner, outer stator/rotor, stator tooth and yoke and stack length are expressed as:

$$0.6 < \frac{D_s}{D_{max}} < 1 \ (D_{max} = 350\ mm), \tag{5}$$

$$0.45 < \frac{D_{s-out}}{D_0} < 0.75, \tag{6}$$

$$0.2 < \frac{D_{s-out}}{D_{s-int}} < 0.6, \tag{7}$$

$$0.5 < \frac{l_o}{l_{amax}} < 1 (l_{a0} = 150\ mm), \tag{8}$$

$$0.2 < \frac{2d_{ys}}{(D_{s-out} - D_{s-int})} < 0.6, \tag{9}$$

$$0.3 < \frac{b_{ts}}{\tau_s} < 0.7, \tag{10}$$

where $D_{s\text{-}out}$ is the outer stator diameter (mm), D_{max} is the maxium diameter (mm), $D_{s\text{-}int}$ is the inner stator diameter (mm), l_o is the stack length, l_{amax} is the maximum stack length, d_{ys} is the yoke thickness to difference between stator outer and inner radius and b_{ts} is the tooth width and τ_s is the slot pitch.

The performances of motor at the base maximum speeds is investigated via the FEM. Namely, the constraints of the minimization problem and objective function values are computed via the optimal design problem that independent variables of the motor are considered. In addition, the information embeded in the optimization procedure is analyzed to iteratively update parameters of the motor and identify different parameters of an optimal motor.

3. Optimization algorithm

An initial modeling and parametric analysis setting for the automatic change of design variables is performed via the FEM embeded in the speed software. By creating Matlab files and batch files, the electromagnetic analysis is automatically performed in the speed software. The obtained results from the FEM will be projected to the Matlab software to define the multi-objective functions and constraints. In addition, when the computational analysis for one experimental point is completed, the shape design parameters are automatically changed in the speed with the aid of CAD tools. As presented, the optimal design of an IPMSM can be considered as a special multi-objective mixed the integer nonlinear problem. According to the multi-objective optimization problem, the FEM is shown that a good approach for the optimal design problem to minimize the sum of the opposites of the electromagnetic torque and weight of the motor.

In general, the multi objective optimization problem can be determined via the vector of parameters [4], [5]:

$$x = [x_1, x_2, \ldots, x_n], \tag{11}$$

for constraint functions: $g_j(x) < 0$ subject to m; boundary constraint (D): $x_{i\_min} < x < x_{i\_max}$; vector function: $f(x) = [f_1(x), f_2(x), \ldots, f_k(x)]$. Thus, one gets:

$$\min f(x);\ g(x) \leq 0;\ \min < x < \max \tag{12}$$

JTE
HCMUTE
ISSN: 2615-9740

JOURNAL OF TECHNICAL EDUCATION SCIENCE
Ho Chi Minh City University of Technology and Education
Website: https://jte.hcmute.edu.vn/index.php/jte/index
Email: jte@hcmute.edu.vn

The obtained solutions from the optimization procedure belong to a Pareto optimal front. On the other hand, the set of vectors of the Pareto front is not dominated by any other vectors. The best design to satisfy the performance criteria is then chosen. The optimization results are given in Table 2.

Table 2. *Optimization results.*

Parameters	min	max	Result 1	Result 2	Result 3	Result 4	Result 5
L1 Magnet Thickness	2	4	3.4272793	2.5130562	2.1064572	2.2644588	2.5225527
L1 Magnet Bar Width	8	12	8.1163493	11.888318	11.746571	9.4149265	8.5429805
L1 Pole V Angle	120	150	134.69761	138.9336	126.55029	149.82566	142.12168
Airgap	0.5	1.5	0.6404491	0.7522818	0.6831523	1.2167976	1.0402752
Stator Lam Dia	130	150	144.76056	142.5347	144.05618	130.56861	134.97574
Stator Bore	70	90	76.629091	80.863833	74.495305	82.988289	83.311474
Tooth Width	4	6	5.7777594	5.6619628	4.3202164	5.351977	5.1164671
Slot Depth	16	20	16.779366	19.544437	17.123348	18.363938	18.102328
Total weighted error			0.0328837	0.0328837	0.0328837	0.0328837	0.0328837

The prototype of proposed IPM motor with a multi objective optimization algorithm has been designed. In order to fit inside the standard aluminum cast frame of the motor manufacturer, the outer diameter of stator has to be fixed. In the same way, the inner diameter rotor has to be fitted with the standard shaft size.

3.1. Step skewing design

The use of step-skewed rotor (SSR) has not been only reduced harmonic components of back EMF, but also minimized the cogging torque and torque ripple. In the electric vehicle (EV) application, in order to decrease torque ripple and increase the torque control precision, the vehicle comfort is thus improved. The no-load and load performances of an IPM motor with the SSR and slot-skewed stator (SSS) have been analyzed and investigated for each motor. The advantage of the step-skew technique is shown in this paper. The obtained results on the performances of each motor are compared to verify between the FEM and experiment method.

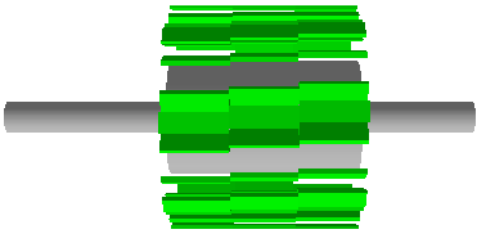

Slice	Proportional	Angle
		Mech Deg
Slice 1	1	-2.5
Slice 2	1	0
Slice 3	1	2.5

Figure 2. *Step-skewed rotor.*

In terms of theory, the torque decreases influence between the step-skew and skew-slot, with the different number of steps. The principle of SSR is pointed out in Figure 2. It can be seen that the harmonic components of back EMF will be reduced. Thus, the step-skew factor ($k_{skew\_pole\_v}$) of harmonic components are expressed [16]- [18]:

JTE
HCMUTE
ISSN: 2615-9740

JOURNAL OF TECHNICAL EDUCATION SCIENCE
Ho Chi Minh City University of Technology and Education
Website: https://jte.hcmute.edu.vn/index.php/jte/index
Email: jte@hcmute.edu.vn

$$k_{skew\_pole\_v} = \frac{sin\left(\frac{n \cdot v \cdot a}{2(n-1)}\right)}{n \cdot sin\left(\frac{v \cdot \alpha}{2(n-1)}\right)} \quad (13)$$

In equation (13), α is the step skew angle, n is the step number and v is the order of harmonic number. In [7], the reduction factors of torque ($k_{T\_skew\_pole\_RE}$) and reluctant torque ($k_{T\_skew\_pole\_PM}$) of step-skewed motor can be presented as [16]-[18]:

$$k_{T\_skew\_pole\_RE} = \frac{sin\left(\frac{n \cdot a}{2(n-1)}\right)}{n \cdot sin\left(\frac{\alpha}{2(n-1)}\right)} = \frac{sin\left(\frac{n \cdot a}{n-1}\right)}{n \cdot sin\left(\frac{\alpha}{n-1}\right)} = k_{T\_skew\_pole\_PM} \cos\left(\frac{\alpha}{2}\right) \quad (14)$$

The torque can be then defined as [15], [16]

$$T = \frac{3}{2} pn \left[\psi_m I_s k_{T\_skew\_pole\_PM} sin\beta + \frac{1}{2} I_s^2 (L_d - L_q) k_{T\_skew\_pole\_RE}\right] sin2\beta, \quad (15)$$

where ψ_m is the magnetic flux per pole of single step, p is the number of pole pair, I_s is the amplitude of stator current and β is the mechanical angle of skewed rotor.

Based on the equation (15), by using the SSR, it can be seen that the PM and reluctant torque components will be reduced. So, the choice of step skew angle and proper step number is very important to decide the power density of motor. The simulated results of back EMF of two prototypes with un-skewed and skewed rotor solved by the FEM with the base speed are shown in Figure 3.

The harmonic components of the proposed motor is indicated in Figure 4. Via the fourier analysis, the harmonic components of order 5, 7, 11 and 23 have appeared with the un-skewed motor. For the step-skewed motor, the magnitude of 5th, 7th and 11th harmonic components has cut, but it is influenced unimportangly on 15th harmonic component. Hence, all these four harmonics has been reduced for the slot-skewed motor. The back EMF results for un-skewed rotor and skewed rotor are given in Table 3. It can be seen that the harmonic distortion of phase voltage for the skewed back EMF is 9.12% where the un-skewed back EMF is 11.52%. This means that for the step skewed rotor, the harmonic component is reduced noticeable. Table 4 gives the results of torque ripple with un-skewed and skewed cases. The obtained result is shown that the torque ripple has reduced from 20.485% to 2.6139%.

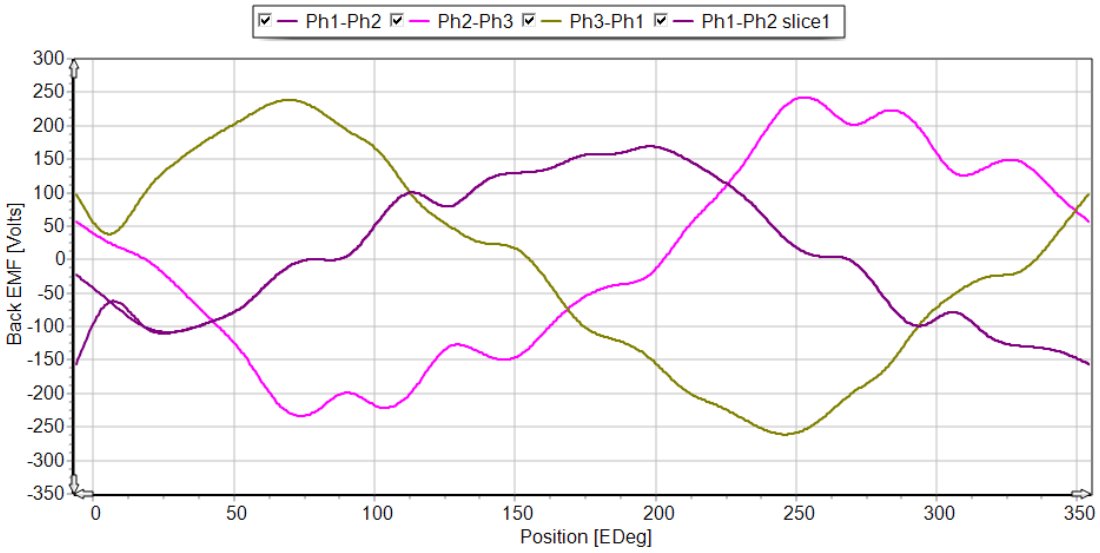

JTE
HCMUTE
ISSN: 2615-9740

JOURNAL OF TECHNICAL EDUCATION SCIENCE
Ho Chi Minh City University of Technology and Education
Website: https://jte.hcmute.edu.vn/index.php/jte/index
Email: jte@hcmute.edu.vn

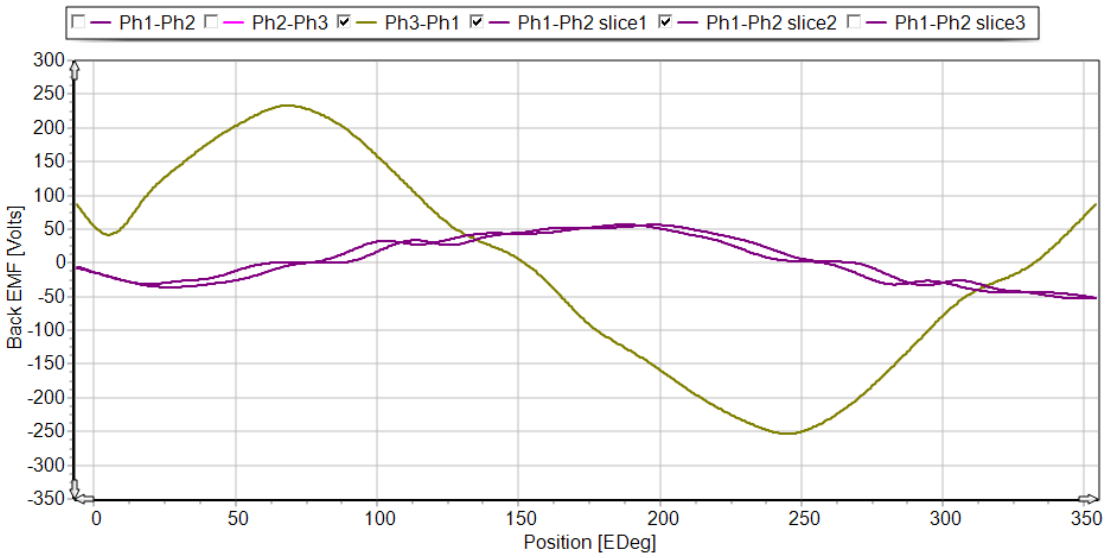

Figure 3. *Un-skewed back EMF (top) and skewed back EMF (bottom).*

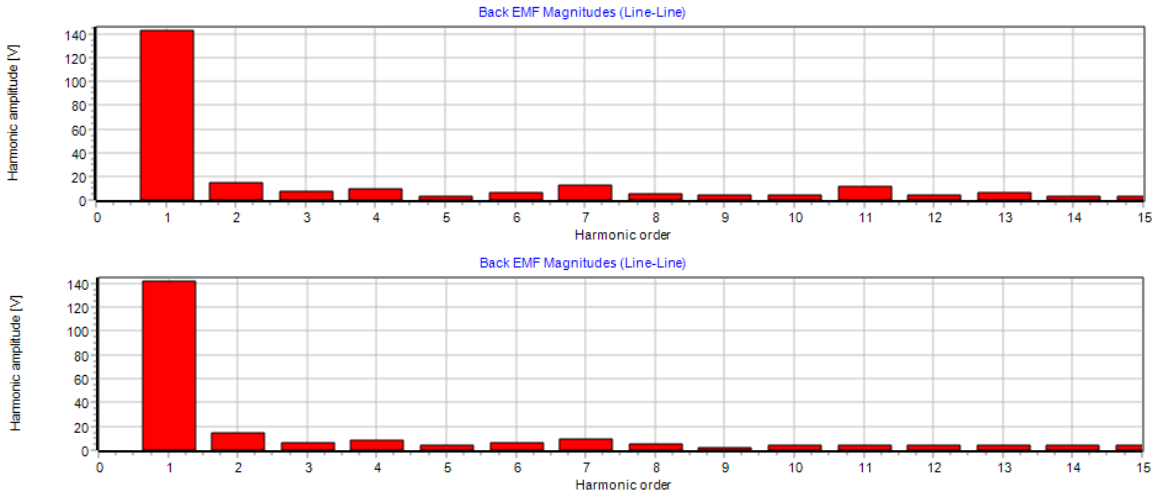

Figure 4. *Harmonic orders of un-skewed EMF (top) and skewed EMF (bottom).*

Table 3. *Back EMF results.*

Parameters	Skewed back EMF	Un-skewed back EMF	Unit
Line-line terminal voltage (rms)	206.6	207.7	Volts
Phase terminal voltage (rms)	120	120.7	Volts
Harmonic distortion line-line terminal voltage	2.548	4.701	%
Harmonic distortion phase terminal voltage	11.19	12.36	%
Back EMF line-line voltage (peak)	123.5	125.3	Volts
Back EMF phase voltage (peak)	77.39	78.31	Volts
Back EMF line-line voltage (rms)	87.56	88.52	Volts
Back EMF phase voltage (rms)	50.74	51.36	Volts
Harmonic distortion back EMF line-line voltage	3.211	5.71	%
Harmonic distortion back EMF phase voltage	9.12	11.52	%
Maximum line-line voltage ratio	1.732	1.732	

Table 4. *Torque ripple results.*

Parameters	Skewed torque ripple	Un-skewed torque ripple	Unit
Average torque (loop torque)	58.706	58.902	Nm
Torque ripple (MsVw)	2.6139	12.146	Nm
Torque ripple (MsVw) [%]	4.4334	20.485	%
Speed limit for constant torque	5022.1	5007.3	rpm
Speed limit for zero torque	68380	72256	rpm
Electromagnetic Power	24697	24836	Watts
Input Power	25462	25602	Watts
Output Power	23818	23959	Watts
Total Losses (on load)	1644.2	1642.1	Watts
System Efficiency	93.542	93.586	%

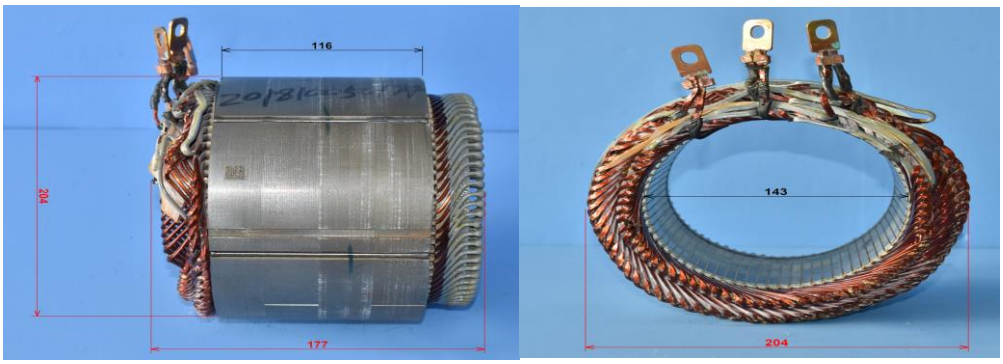

Figure 5. *Assembled stator.*

Finally, the product of stator lamination is manufactured and assembled as shown in Figure 5. The hairpin windings are also done in the stator slots.

4. Conclusions

The prototype of opitimzaition procedure has been verified and developed with the effective analytical model. An intelligent optimization algorithm has been fully proposed in a very short period without using the FEM. The obtained results from the optimizaiton approach have been presented the efficiency of the proposed technique. The combination of optimization program and analytical model is performed in the source-code Matlab that make it easier to use. The requirements and boundaries are truly suggested to validate the IPM motor. The obtained results have been verified with the FEM controlled via the Matlab program which can be considered as an excellent powerful tool for the optimized design of a IPMSM. The performances of IPMSM has been successfully improved via the technique of SSR due to the reduction of harmonics of back EMF from 11.52% (with un-skewed) to 9.12% (with skewed) and torque ripple from 20.485% (with un-skewed) to 2.6139% (skewed).

In addition, this technique has also allowed to reduce the time on embedding wires. It will be an important trend on mass production of IPM traction motors with application to EVs.

Acknowledgments

This research is funded by Hanoi University of Science and Technology under project number T2022-PC-009.

REFERENCES

[1] B. M. Dinh, B. D. Hung, T. V. Linh, and D. Q. Vuong, "Improved Torque and Efficiency of Induction Motors by Changing Rotor Structure of Permanent Magnet Assistance Synchronous Reluctance Motors," *Journal of Technical Education Science*, no. 71A, pp. 1–7, 2022, doi: https://doi.org/10.54644/jte.71A.2022.1145.

[2] B. D. Hung, B. M. Dinh, and D. Q. Vuong, "Performance Improvement of IPM Motors by Change of Rotor Shapes-Application to Electric Vehicles," *Journal of Military Science and Technology*, no. 83, pp. 1-10, Nov. 2022, doi:10.54939/1859-1043.j.mst.83.2022.1-10.

[3] B. M. Dinh, N. H. Phuong, D. Q. Vuong, and B. D. Hung, "Electromagnetic and Thermal Analysis of Interior Permanent Magnet Motors Using Filled Slots and Hairpin Windings", *Eng. Technol. Appl. Sci. Res*., vol. 12, no. 1, pp. 8164–8167, Feb. 2022.
[4] G. Hong, T. Wei and X. Ding, "Multi-Objective Optimal Design of Permanent Magnet Synchronous Motor for High Efficiency and High Dynamic Performance," *IEEE Access*, vol. 6, pp. 23568-23581, 2018, doi: 10.1109/ACCESS.2018.2828802.
[5] S. O. Edhah, J. Y. Alsawalhi and A. A. A. Durra, "Multi-Objective Optimization Design of Fractional Slot Concentrated Winding Permanent Magnet Synchronous Machines," *IEEE Access*, vol. 7, pp. 162874-162882, 2019, doi: 10.1109/ACCESS.2019.2951023.
[6] J. H. Lee *et al*., "A Novel Memetic Algorithm Using Modified Particle Swarm Optimization and Mesh Adaptive Direct Search for PMSM Design," *IEEE Transactions on Magnetics*, vol. 52, no. 3, pp. 1-4, Mar. 2016, doi: 10.1109/TMAG.2015.2482975.
[7] S. Zhang, W. Zhang, R. Wang, X. Zhang and X. Zhang, "Optimization design of halbach permanent magnet motor based on multi-objective sensitivity," *CES Transactions on Electrical Machines and Systems*, vol. 4, no. 1, pp. 20-26, Mar. 2020, doi: 10.30941/CESTEMS.2020.00004.
[8] L. Zhai, T. Sun and J. Wang, "Electronic Stability Control Based on Motor Driving and Braking Torque Distribution for a Four In-Wheel Motor Drive Electric Vehicle," *IEEE Transactions on Vehicular Technology*, vol. 65, no. 6, pp. 4726-4739, Jun. 2016, doi: 10.1109/TVT.2016.2526663.
[9] X. Zhu, Z. Shu, L. Quan, Z. Xiang and X. Pan, "Design and Multicondition Comparison of Two Outer-Rotor Flux-Switching Permanent-Magnet Motors for In-Wheel Traction Applications," *IEEE Transactions on Industrial Electronics*, vol. 64, no. 8, pp. 6137-6148, Aug. 2017, doi: 10.1109/TIE.2017.2682025.
[10] W. Fei, P. C. K. Luk, D. M. Miao and J. X. Shen, "Investigation of Torque Characteristics in a Novel Permanent Magnet Flux Switching Machine With an Outer-Rotor Configuration," *IEEE Transactions on Magnetics*, vol. 50, no. 4, pp. 1-10, Apr. 2014, doi: 10.1109/TMAG.2013.2288219.
[11] Y. Fan, L. Zhang, J. Huang and X. Han, "Design, Analysis, and Sensorless Control of a Self-Decelerating Permanent-Magnet In-Wheel Motor," *IEEE Transactions on Industrial Electronics*, vol. 61, no. 10, pp. 5788-5797, Oct. 2014, doi: 10.1109/TIE.2014.2300065.
[12] Y. Wang, H. Fujimoto and S. Hara, "Driving Force Distribution and Control for EV With Four In-Wheel Motors: A Case Study of Acceleration on Split-Friction Surfaces," *IEEE Transactions on Industrial Electronics*, vol. 64, no. 4, Apr. 2017, pp. 3380-3388, doi: 10.1109/TIE.2016.2613838.
[13] C. C. Hwang and Y. H. Cho, "Effects of leakage flux on magnetic fields of interior permanent magnet synchronous motors," *IEEE Transactions on Magnetics*, vol. 37, no. 4, pp. 3021-3024, Jul. 2001, doi: 10.1109/20.947055.
[14] R. Ilka *et al.*, "Techno-economic Design Optimisation of an Interior Permanent Magnet Synchronous Motor by Multi-objective approach," *IET Electric Power Applications*, vol. 12, 2018, doi: 10.1049/iet-epa.2018.0150.
[15] G. Hong, T. Wei and X. Ding, "Multi-Objective Optimal Design of Permanent Magnet Synchronous Motor for High Efficiency and High Dynamic Performance," *IEEE Access*, vol. 6, pp. 23568-23581, 2018, doi: 10.1109/ACCESS.2018.2828802.
[16] S. K. Cho *et al*., "Design Optimization of Interior Permanent Magnet Synchronous Motor for Electric Compressors of Air-Conditioning Systems Mounted on EVs and HEVs," *IEEE Transactions on Magnetics*, vol. 54, no. 11, pp. 1-5, Nov. 2018, doi: 10.1109/TMAG.2018.2849078.
[17] A. J. P. Ortega, S. Paul, R. Islam and L. Xu, "Analytical Model for Predicting Effects of Manufacturing Variations on Cogging Torque in Surface-Mounted Permanent Magnet Motors," *IEEE Transactions on Industry Applications*, vol. 52, no. 4, pp. 3050-3061, Aug. 2016, doi: 10.1109/TIA.2016.2554102.
[18] Y. Zhou, H. Li, G. Meng, S. Zhou and Q. Cao, "Analytical Calculation of Magnetic Field and Cogging Torque in Surface-Mounted Permanent-Magnet Machines Accounting for Any Eccentric Rotor Shape," *IEEE Transactions on Industrial Electronics*, vol. 62, no. 6, pp. 3438-3447, Jun. 2015, doi: 10.1109/TIE.2014.2369458.

Dr. Bui Duc Hung is currently working as a team leader of electrical machines's group, and also a lecturer of Department of Electrical Engineering, School of Electrical Engineering, Hanoi University of Science and Technology. He obtained the PhD degree in the Department of Electrical Engineering, Hanoi University of Science and Technology, in 2000.

Dr. Bui Minh Dinh is currently working as a lecturer at Department of Electrical Engineering, School of Electrical and Electronic Engineering, Hanoi University of Science and Technology. He obtained the PhD degree in the Department of Electrical Engineering, TU university, in 2014.

Assoc. Prof. Dang Quoc Vuong is currently a deputy director of Training Center of Electrical and Electronic Engineering, and also a lecturer of Department of Electrical Engineering, School of Electrical Engineering, Hanoi University of Science and Technology. He obtained the PhD degree in the Electrical Engineering and Computer Science Department of the University of Liège, Belgium, in 2013.